Int. J. Multiphase Flow, Vol. 2, pp. 19–33. Pergamon Elsevier, 1975. Printed in Great Britain.

METHODS FOR CALCULATING TRACER DISTRIBUTION IN MULTIPHASE PLUG FLOW SYSTEMS

J. REISS*, J. DAYAN† and D. RAPPAPORT*

Technion Israel Institute of Technology, Haifa, Israel

(*Received* 11 *June* 1974)

Abstract—A novel continuous time and space Monte Carlo simulation technique is presented for solving equations describing tracer distribution in multiphase inhomogeneous plug-flow systems. Comparison is made with the commonly employed method of characteristics. This comparison indicates that the method of characteristics is unreliable for systems with spacially varying parameters. Further, results indicate that the suggested Monte Carlo technique is more efficient in the use of computer time than the method of characteristics. Examples are given.

1. INTRODUCTION

This work describes two methods (the method of characteristics and a Monte Carlo simulation technique) for simulation of certain transport processes, in which the material entering a zone of interest (the system) is transported through it in one or more of distinct phases.

Each phase is a plug flow phase with constant volumetric flow rate. However, the cross-section area may vary along the system and thus a characteristic "velocity profile" $f_i(x)$ which varies with phase (i) or spatial location (x), can be defined.

Material within the system may be transported in the same phase to the system boundary, or it may transfer anywhere along the way into another phase travelling possibly in the opposite direction (x is assumed scalar). Such a transfer may occur at any point along the path, in accordance with exchange coefficient profiles $\lambda_{ij}(x)$ for transfer between phases i and j. Note that λ_{ij} may vary throughout the system. The effect of dispersion due to molecular diffusion anywhere in the system or its boundaries is not considered.

In the characteristics method of simulation, partial differential equations for material balance within the system are solved to give the material concentrations at any x and t. The Monte Carlo simulation technique described here is a novel method, very efficient and accurate and much less computer-time consuming than the classical characteristic method. The method, based on Rappaport & Dayan (1973), solves for the concentrations by introducing a large number of tracer particles into the system and tracing their trajectories as they travel through the system. These trajectories are generated randomly in accordance with probability distributions derived from the stochastic process associated with the material balance equations. For both methods simulation programs were written to provide the material distribution of a given system (specified by "velocity profiles" and exchange coefficients for each phase) at any x and t. For the purpose of comparing these two methods only the residence time distribution (overall time distribution of material at the system exit) is given here. In addition, these results can be compared with experimental results obtained from real systems which can be described by such a model, and thus provide confirmation of the model used, or help predict the system behavior when different parameters in the model are changed.

Previous work on the subject includes derivations of the Monte Carlo and characteristics solutions for the case of spatially constant systems (Dayan & Levenspiel 1970), which this work expands to cover the spatially varying case. The numerical examples are based on the Kunii & Levenspiel (1969) model for a fluidized bed. Another possible flow model is

* Electrical Engineering Department.
† Mechanical Engineering Department.

that of the spouted bed. Both the fluidized bed and the spouted bed systems were described by Dayan *et al.* (1973).

2. MATHEMATICAL DISCUSSION

The considered system consists of m plug flow phases each of which flows with velocity $f_i(x)$ for phase i. When deriving the material balance equation we assume a conservative mass system with no gain or loss of material in it. Flows in and out occur only at the end boundaries, $x = 0$ and $x = x_{max}$, and diffusion plays no role anywhere in the system, as mentioned. A phase i is called a forward (backward) phase if $f_i > 0$ ($f_i < 0$) and a stagnant phase if $f_i = 0$. The tracer material is introduced into the system at $t = 0$.

Material introduced into phase i is transported in it at the phase velocity. At each point along the path a certain proportion of the material transfers into other phases and from each of the other phases back into phase i. The material exchange between phases seen by an observer moving at the phase velocity in phase i is (defining x_t as the position of the observer at time t):

$$\frac{d}{dt}(C_i(x_t, t)) = \sum_{j=1}^{m} \lambda_{ji}(x_t)C_j(x, t) - \lambda_{ij}(x_t)C_i(x, t) \qquad [1]$$

where $\lambda_{ij}(x)$, in units ($\sec^{-1}$), is the rate of exchange of material from phase i to phase j, $\lambda_{ii}(x) = 0$, and $\lambda_{ij}(0) = 0$ ($\lambda_{ij}(x_{max}) = 0$) for i a forward (backward) phase. $C_i(x, t)$ is the concentration of material (per unit length) in phase i at coordinates (x, t) and $\Delta x = f_i(x)t$. These equations (for $i = 1, 2, \ldots, m$) can be rewritten as the following set of partial differential equations

$$\frac{\partial C_i(x, t)}{\partial t} = -\frac{\partial[f_i(x)C_i(x, t)]}{\partial x} + \sum_{j=1}^{m} \lambda_{ji}(x)C_j(x, t) - \sum_{j=1}^{m} \lambda_{ij}(x)C_i(x, t). \qquad [2]$$

These equations must be solved to determine $C_i(x, t)$, the tracer concentration in the system at any point (x, t) of phase i.

The (RTD) for forward phases is

$$\mathrm{RTD}(t) = \sum_{i=1}^{m} C_i(x_{max}, t) \qquad [3]$$

and for backward phases is

$$\mathrm{RTD}(t) = \sum_{i=1}^{m} C_i(0, t).$$

Note that as a result of the assumptions on the exchange coefficients $C_i(0, t) = 0$, ($C_i(x_{max}, t) = 0$) for $t > 0$, for i a forward (backward) phase. To solve the above set of partial hyperbolic differential equations we shall discuss the classical method of characteristics first.

In our simulation, [2] was solved for the case of two phases. The method is general, however, and can be extended to any number of phases.

Consider the set of equations:

$$\Delta \equiv \begin{bmatrix} 1 & 1 & 0 & 0 \\ 0 & 0 & 1 & 1 \\ f_1\,dt & dx & 0 & 0 \\ 0 & 0 & f_2\,dt & dx \end{bmatrix} \cdot \begin{bmatrix} \frac{\partial C_1}{\partial t} \\ \frac{\partial(f_1C_1)}{\partial x} \\ \frac{\partial C_2}{\partial t} \\ \frac{\partial(f_2C_2)}{\partial x} \end{bmatrix} = \begin{bmatrix} \lambda_{21}C_2 - \lambda_{12}C_1 \\ \lambda_{12}C_1 - \lambda_{21}C_2 \\ d(f_1C_1) \\ d(f_2C_2) \end{bmatrix} \triangleq \begin{bmatrix} A \\ B \\ d(f_1C_1) \\ d(f_2C_2) \end{bmatrix} \qquad [4]$$

where for brevity we substitute C_i for $C_i(x, t)$, f_i for $f_i(x)$, etc., and where A and B are defined by this equation.

The first two lines in [4] are the partial differential equations [2]. The following two lines are partial derivative expansions of the differentials $d(f_1C_1)$ and $d(f_2C_2)$ in terms of dx and dt.

The method of characteristics changes the above partial differential equations into ordinary differential equations which must, however, be integrated in particular directions. These characteristic directions are those for which the matrix determinant is zero, namely, $dx/dt = f_1$, or $dx/dt = f_2$.

If the determinant of the square matrix in [4] is zero, substituting the right hand side of the equation for any one of the matrix columns will still give a zero determinant. Substituting for the second column of Δ and choosing $dx/dt = f_1$, $(f_1 \neq f_2)$, we obtain:

$$\frac{d(f_1C_1)}{dx} = A = \lambda_{21}C_2 - \lambda_{12}C_1 \qquad [5]$$

with $dx/dt = f_1$ as the direction of integration. Substituting for the fourth column of Δ and choosing $dx/dt = f_2$(again $f_1 \neq f_2$), we obtain:

$$\frac{d(f_2C_2)}{dx} = B = \lambda_{12}C_1 - \lambda_{21}C_2 \qquad [6]$$

with $dx/dt = f_2$ as the direction of integration. Note that the two equations are interconnected. To solve for $d(f_1C_1)/dx$ we must know C_2, and similarly to solve for $d(f_2C_2)/dx$ we must know C_1. Also, since the integration of each equation proceeds in a different direction, we cannot simply alternately solve for successive increments in C_1 and C_2. In fact we have a network of intersecting coordinates over the (x, t) plane, as is shown in figure 1 for the cocurrent case and in figure 2 for the countercurrent case.

For the cocurrent case the darkened lines in figure 1 represent the (x, t) coordinates of particles travelling only in phase 1 or only in phase 2. Along the darkened line marked "Pure C_1" the concentration C_2 is known to be zero, while along the "Pure C_2" line the concentration C_1 is zero. As this removes the coupling between the differential equations, we can solve analytically for C_1 along the "Pure C_1" line and for C_2 along the "Pure C_2" line. In general to obtain the integral form of these differential equations we proceed as follows:

$$\text{For } \frac{dx}{dt} = f_1\text{: } \frac{d}{dx}(f_1C_1) = \frac{\lambda_{21}(f_2C_2)}{f_2} - \frac{\lambda_{12}(f_1C_1}{f_1} \qquad [7]$$

$$\text{For } \frac{dx}{dt} = f_2\text{: } \frac{d}{dx}(f_2C_2) = \frac{\lambda_{12}(f_1C_1)}{f_1} - \frac{\lambda_{21}(f_2C_2)}{f_2}. \qquad [8]$$

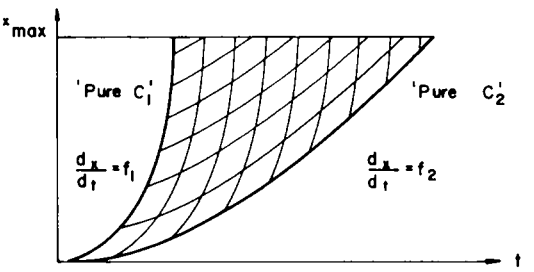

Figure 1. Characteristic curves for cocurrent case.

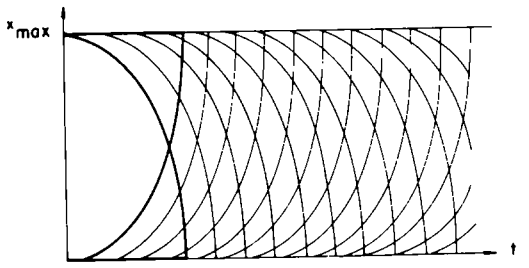

Figure 2. Characteristic curves for countercurrent case.

Denoting t along the integration path as t_u, and integrating along $dx/dt = f_1$ from the starting point (x_o, t_o), we get:

$$f_1(x)C_1(x,t) = \exp\left(-\int_{x_o}^{x}\frac{\lambda_{12}(u)}{f_1(u)}du\right) \cdot\left[\int_{x_o}^{x}\left\{\exp\left[\int_{x_o}^{u}\frac{\lambda_{21}}{f_1(v)}(v)\,dv\right]\lambda_{21}(u)C_2(u,t_u)\,du\right\} + f_1(x_o)C_1(x_o,t_o)\right] \quad [9]$$

and along $dx/dt = f_2$:

$$f_2(x)C_2(x,t) = \exp\left(-\int_{x_o}^{x}\frac{\lambda_{12}(u)}{f_2(u)}du\right) \cdot\left[\int_{x_o}^{x}\left\{\exp\left[\int_{x_o}^{u}\frac{\lambda_{21}}{f_2(v)}(v)\,dv\right]\lambda_{12}(u)C_1(u,t_u)\,du\right\} + f_2(x_o)C_2(x_o,t_o)\right] \quad [10]$$

where x_o is the starting point for the integration.

Equations [9] and [10] are integrated over different paths leading to the point whose solution we wish to determine.

Note that $C_2(u, t_u) = 0$ for all u along the path of integration so that [9] becomes:

Along $dx/dt = f_1$, where $C_2(u, t_u) = 0$

$$f_1(x)C_1(x,t_x) = f_1(x_o)C_1(x_o,t_{x_o})\exp\left(-\int_{x_o}^{x}\frac{\lambda_{12}(u)}{f_1(u)}du\right) \quad [11]$$

and [10] becomes, for $C_1(u, t_u) = 0$ along its integration path:

$$f_2(x)C_2(x,t_x) = f_2(x_o)C_2(x_o,t_{x_o})\exp\left(-\int_{x_o}^{x}\frac{\lambda_{21}(u)}{f_2(u)}du\right). \quad [12]$$

This then is the previously mentioned analytic solution along the darkened lines in figure 1.

We see that falling exponentials are a commonly occurring form in these equations. This is used in the integration procedure, where an analytic form for C_2 must be assumed during the integration for C_1. The analytic form chosen was an exponential form.

Figure 2 describes the characteristics grid for a general case of countercurrent two phase flow system, i.e. the injection of transferable material simultaneously in both phases (at $x = 0$ and $x = x_{max}$) and, of course, where f_1, f_2, λ_{12}, λ_{21}, are all x dependent. It is seen from figure 2 that the integration of the differential equations for the countercurrent case is more complicated than for the cocurrent case. In fact the cocurrent method of integration described by Reiss (1974) cannot be applied here.

The countercurrent case has been programmed by Dayan (1968) using the method of characteristics for the constant coefficients case, where all the transferable material enters

the system through one phase only (say, at $x = 0$). This eliminates the upper triangle grid of figure 2, and, of course, the characteristic lines of this figure are all straight lines (constant velocities and constant transfer coefficients throughout the system). There should be no hindrance to the development of a general procedure of integration for the general case of countercurrent flow system on a point by point basis, where successive points are found by integration from a pair of previous points. However, based on the conclusions derived from the comparison of the cocurrent case solutions (by the method of characteristics) to the herewith suggested (Monte Carlo) method it was already clear that this is not worth the effort. Moreover, because of the non-linearity of the characteristic lines, there is the danger that an iterative method would tend to bunch the generated points and not cover the entire (x, t) plane effectively.

Next we shall present the novel Monte Carlo method to solve the set [2].

As in other Monte Carlo simulation techniques a large number of "particles" is injected into the system to simulate the transported tracer material. Each one of these particles follows a certain path through the system (we randomly specify a jump from phase to phase at different times and locations). While in a certain phase it is assumed that these tracer particles travel at the same velocity and have the same interphase exchange coefficients as the actual material transported in the system. The exchange coefficients specify jump probabilities for the particles and from these probabilities together with the known phase velocity a probability distributions for the length of stay in each of the phases can be derived. As the particle velocities and jump probabilities (exchange coefficients) are x dependent only and previous history has no effect whatsoever on the coming steps, the described process is a Markov process (Rappaport & Dayan 1973).

Recording the position of each particle at selected times gives the particle distribution within the system as a function of time. The distribution of the times needed for the particles to exit the system is the RTD.

The jump probabilities are derived formally as follows: consider tracer particles in phase i at (x_o, t_o). These particles travel on the trajectory $\dot{x}_t = f_i(x_t, t)$.

For such particles the *loss* from phase i along the trajectory on some small time interval is approximated by:

$$\frac{\mathrm{d}}{\mathrm{d}t} C_i(x_t, t) = -\sum_{j=1}^{m} \lambda_{ij}(x_t) C_i(x_t, t). \qquad [13]$$

Note that this is simply the homogeneous part of the ordinary differential equation [1] for the time change in C along the trajectory. Integrating,

$$C_i(x_t, t) = C_i(x_o, t_o) \exp\left(-\int_{t_o}^{t} \sum_{j=1}^{m} \lambda_{ij}(x_s)\, \mathrm{d}s \right) \qquad [14]$$

where x_s is $x(t)$ along the integration path ($t = s$). Thus, of the original particles at point (x_o, t_o):

$$\frac{C_i(x_t, t)}{C_i(x_o, t_o)} = \exp\left(-\int_{t_o}^{t} \sum_{j=1}^{m} \lambda_{ij}(x_s)\, \mathrm{d}s \right) \qquad [15]$$

is the fraction which remains in phase i at point (x, t).

Thus, the probability of remaining in phase i on interval (t_o, t) given that the particle at time t_o is at x_o, is:

$$\Pr(\text{no jump on } (t_o, t) \mid x_o) = \exp\left(-\int_{t_o}^{t} \sum_{j=1}^{m} \lambda_{ij}(x_s)\, \mathrm{d}s \right). \qquad [16]$$

From the definition of the exchange coefficients, we conclude that the probability of jumping from phase i to phase $k \neq i$ is:

$$\Pr(\text{jump from } i \text{ to } k \text{ on } (t_o, t)|x_o) \simeq \lambda_{ik}(x_o)(t - t_o). \quad [17]$$

We can further determine, given the fact that a jump has occurred at $[x, t]$ the probability for jumping into any other phase $k \neq i$:

$$P_{ik}(x, t) = \lim_{\Delta t \to 0} \frac{\Pr(\text{jump from } i \text{ to } k \text{ on } (t, t + \Delta t)|x)}{\Pr(\text{jump from } i \text{ on } (t + \Delta t)|x)} \quad [18]$$

where $\Delta x = f(x, i)\Delta t$.

From [16] and [17]

$$P_{ik}(x, t) = \frac{\lambda_{ik}(x, t)}{\sum_{j=1}^{m} \lambda_{ij}(x, t)}. \quad [19]$$

Thus, we have all the probability distributions we need to generate our tracer particle trajectories for the Monte Carlo method.

Note that the above probabilities are given in terms of path integral, that is unlike other Monte Carlo simulation techniques where all probabilities are calculated at present locations or time periods resulting from arbitrary division (discretizing) of the entire space. Thus a novel continuous time and space technique is suggested which eliminates the artificial nature of the familiar techniques.

We shall now explain the method of generating the particle trajectories. Assume we have generated the trajectory up to time t_o and point x_o and the particle has just jumped at (t_o, x_o) to phase i. The next point of jump of the particle out of phase i is generated in accordance with the above described probabilities. This is done by generating a random variable X, the next jump location, whose probability distribution is given by:

$$\Pr(X < x) = 1 - \exp\left(- \sum_{j=1}^{m} \int_{x_o}^{x} \frac{\lambda_{ij}(y)\, dy}{f_i(y)} \right). \quad [20]$$

Equation [20] is derived from [16] by a change of variable and the law of conservation of probabilities.

The time to the next jump is simply that required to reach x from x_o on the trajectory in phase i starting from (x_o, t_o).

A common technique (see, for example, Himmelblau (1970)) is used to modify a random number, RN, having a uniform probability density over the interval (0, 1) into a random variable $F^{-1}(RN)$ with the required probability distribution $F(x) = Pr(X < x)$.

The procedure for generating the next projected jumping point is to generate the uniform random variable RN, and then to find $F^{-1}(RN)$, (a table-search technique can be used). If the jumping point is outside the system boundaries, we truncate the trajectory at the boundary and calculate the residence time for the particle. Otherwise we pick the phase to which the particle will jump, again using the random number generator and the probabilities of [19].

At this stage we have a new initial point, a new time coordinate, and a new phase, so we can proceed to generate the remainder of the particle trajectory from these new starting points.

The assumption of forward flow in the above derivation does not detract from its generality. In the computer program implementation, flow can be assumed positive for all phases, and a transformation of coordinates can be made when jumping between phases of different directions.

The Monte Carlo method can be interpreted in terms of the characteristic lines. To do this we substitute for the concept "normalized concentration of material at (x, t)", the prob-

abilistic equivalent "probability that a single particle will be found at x at time t". The particles move in the characteristic directions $\dot{x} = f_i(x, t)$. If we generate a large number of trajectories according to the probabilities of [17] and [19], we tend to cover the (x, t) plane with these trajectories with a density proportional to the probability of a particle being at (x, t).

Equations [11] and [12] for the concentration of material in the "Pure C_1" and "Pure C_2" curves are similar to the Monte Carlo probability for a tracer particle to remain in its initial phase without jumping ([16]). The differences between these equations and [16] are due to the fact that [16] is an integration in t, while [11] and [12] are integrations in x.

The application of the usual type of random walk techniques requires the building of a fine space grid on which the typical particle moves from one intersection to another. Note that this is fundamentally similar to the building of the time-space grid for the solving of the above partial differential equations by the method of characteristics. In both these cases, theoretically speaking, the finer the grid the closer the calculated solution is to the actual solution of the partial differential equations. For the sake of argument let us call the above procedures grid decision ones.

In contrast, for the jump process described above, the mean number of jumps which a typical particle undergoes on some finite time interval is finite as is also the standard deviation about this mean. The significance of this is that the number of decisions (i.e. jumps) that the typical particle makes is *considerably fewer than that involved* in the grid-decision procedures. This accounts for the fact that the computation time needed for reasonable solutions by the simulation technique suggested by the authors is less than that needed for the grid-decision procedures (see the numerical example). Further, the probability formula [18] indicates that the proper partitioning of the grid for the grid-decision procedures is one that will correspond to equal probability of jump from grid point to grid point. This means at point (x, t), for example, in the method of characteristics, the grid points (i.e. the intersection points of the various characteristic curves), should be spaced on the x-axis at distances proportional to $\lambda_{ij}(x)/f_i(x)$. However, this results in a different x quantization for each phase. This situation is highly impracticable.

NUMERICAL EXAMPLE

The following example is given here merely for the sake of comparing the method of characteristics and the newly suggested Monte Carlo method in order to point out the advantages of the latter. The physical system chosen for these calculations is the fluidized bed system, in which, to our understanding, it is possible to describe the pattern of gas flow by means of a two phase plug flow model. As it is not the purpose of this paper to justify the adequacy of such a model for this system, no attempt was made to compare the RTD curves obtained from the calculations to any real experimental data.

Let us discuss the two regional models for fluidized bed first. In a series of articles, later summarized in their book, Kunii & Levenspiel (1969) proposed a simple one-parameter model for a fluidized bed. Calculation of all bed variables was based on this single parameter —the equivalent bubble diameter. In this model gas flows through two cocurrent "phases", the "bubble phase" and the "emulsion phase". Under certain flow conditions ($u_o/u_{mf} > 6 \div 11$) the emulsion phase reverses itself and flows downwards, counter to the uprising bubbles. It is assumed in the original KL (Kunii and Levenspiel) model, among other things, that the flow of gas is plug-flow in both phases and that due to breakage and coalescense the size of bubbles remains constant along the bed. RTD curves for the original KL model with the constant bubble size assumption were first calculated using the Method of Characteristics by Yoshida & Kunii (1968) and by Dayan & Levenspiel (1970). A possibly more realistic model with varying bubble size can be derived as follows (for nomenclature refer to figure 3).

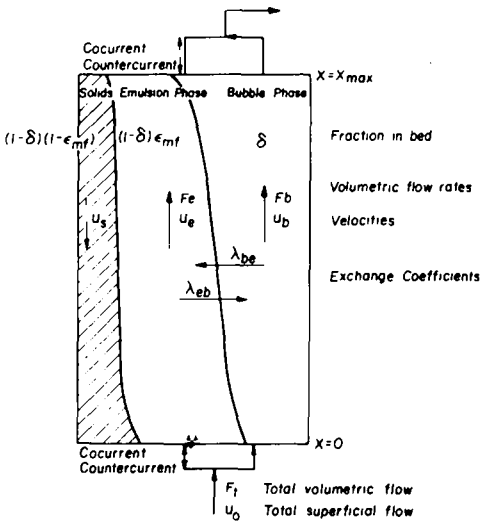

Figure 3. Schematics of the fluidized bed model.

The single-bubble velocity in the bed is given by Davidson & Harrison (1963).

$$u_{br} = 0.711(gd_{br})^{1/2}. \qquad [21]$$

Obviously a large bubble rises faster than a small one. It is known that bubbles grow as they rise in the bed. They also grow when the input gas velocity is increased (Kobayashi & Arai 1964; Kunni & Levenspiel 1969, p. 185).

The single bubble velocity is related to the bubble phase velocity through (Kunii & Levenspiel 1969, pp. 154, 161):

$$u_b = u_o - u_{mf} + 0.711(gd_{br})^{1/2}. \qquad [22]$$

This was derived from the equation for δ—the bubble fraction in the bed

$$\delta = \frac{u_o - u_{mf}}{u_b - u_{mf}}. \qquad [23]$$

The emulsion gas velocity is given by

$$u_e = \frac{u_{mf}}{\varepsilon_{mf}} - u_s \qquad [24]$$

where

$$u_s = \frac{\alpha\delta u_b}{1 - \delta - \alpha\delta} \qquad [25]$$

can be calculated from [23]. α, which is defined as (volume of wake/volume of bubble), is a constant between $0.25 \div 0.4$ as was given by Orcutt (1960). Knowing the change of d_{br} along the bed, u_b and u_e at all bed levels can be calculated from the above equations. Kunii & Levenspiel (1969) state that for $u_o/u_{mf} > 2$ only large fast bubbles with negligible clouds may be expected in the bed. For such bubbles the exchange coefficients are given by the following equations:

$$\lambda_{bc} \simeq 4.5\frac{u_{mf}}{d_{br}} + 5.85\frac{\mathscr{D}_{eq}^{1/2}g^{1/4}}{d_{br}^{5/4}} \qquad [26]$$

$$\lambda_{ce} \simeq 6.78\left(\frac{\varepsilon_{mf}\mathscr{D}_{eq}u_b}{d_{br}^3}\right)^{1/2} \qquad [27]$$

$$\lambda_{be} = \left(\frac{1}{\lambda_{bc}} + \frac{1}{\lambda_{ce}}\right)^{-1} \qquad [28]$$

$$\lambda_{eb} = \frac{\lambda_{be} \cdot \delta}{(1 - \delta)\varepsilon_{mf}} \quad [29]$$

where $e_{mf}\mathscr{D} < \mathscr{D} < \mathscr{D}_{eq}$ ($\mathscr{D}$ = molecular diffusion of tracer material).

For the cocurrent flow case ($u_o/u_{mf} > 6 \div 11$) tracer injected at the distributor is divided between the bubble phase and the emulsion phase in accordance with the ratios p_b and p_e, where

$$p_b = \frac{F_b}{F_b + F_e} = \frac{F_b}{F_t} = \frac{u_o - u_{mf}(1 - \delta)}{u_o} \quad [30]$$

$$p_e = 1 - p_b. \quad [31]$$

For countercurrent flow all the material is injected into the upwards flowing (bubble) phase. A certain fraction of the material exiting at $x = x_{\max}$ is sucked back into the downwards flow and does not leave the system. This fraction is the ratio of volumetric flow rates, p_r, or:

$$p_r \text{ (suction back into system)} = \frac{(1 - \delta)\varepsilon_{mf}}{\delta + (1 - \delta)\varepsilon_{mf}}. \quad [32]$$

There are a few studies of changes in bubble size along the bed and the effect of gas velocity on these changes. For the present example the Kato & Wen (1969) relationship was taken (see also Fryer & Potter 1972):

$$d_{br} = (d_{br})_{x=0} + mx \quad [33]$$

where $(d_{br})_{x=0}$ is the size at the distributor and m is given by Kobayashi *et al.* (1966) as

$$m = 1.4(d_p\rho_s)\frac{u_o}{u_{mf}}. \quad [34]$$

No check for maximum stable bubble diameter has been made in this study. Since a value of δ greater than 0.5 was considered unrealistic, d_{br} was not allowed to go below the value which results in $\delta = 0.5$ in our simulation.

Table 1 summarizes all the data necessary to calculate the RTD for a hypothetical fluidized bed filled with microspherical catalyst (Hiraki *et al.* 1965). Air at atmospheric conditions was used as the fluidized agent and helium ($\mathscr{D} = 0.71$ cm^2/sec) was used as the non-absorbed tracer for the RTD study. The u_o/u_{mf} ratios for both cocurrent and countercurrent cases imply large fast bubbles with negligible cloud.

Table 1. Data for calculations of RTD in fluidized bed

Material	Microspherical Catalyst
Fluid	Air (at atmospheric pressure)
d_p[mm]	0.15
$\rho_s[\frac{gr}{cm^3}]$	1.54
$u_{mf}[\frac{cm}{sec}]$	3.4
ε_{mf}	0.5
α	0.3
$(d_{br})_{z=0}$[cm]	2.0 (estimated)
L[cm]	100.0
u_o/u_{mf}	2 (giving cocurrent flow) 14 (giving countercurrent flow)

In the course of calculations we have made several assumptions (which can be easily modified as better physical data or relationships become known, without affecting the method of calculation):

(1) $\varepsilon_{mf} = 0.5$ was used where no other relations are given.
(2) α was estimated as in Kunii & Levenspiel (1969, Ch. 5).
(3) $\mathscr{Q}_{eq} = \mathscr{Q}$.
(4) The height of the fluidized bed does not change much with changes in u_o.

RTD for the above described fluidized bed model was calculated by both methods.

RESULTS AND CONCLUSIONS

The fluidized bed example provides highly non-linear expressions for the system parameters $\lambda(x)$'s and $f(x)$'s. Thus, these parameters were precalculated in several points along the system (at several x's) and stored in the computer in the form of tables.

In the computation of the distribution by the Monte Carlo program, and in the integrations of the characteristics program, it was assumed that the values of the system parameters λ and f remained constant over each interval of the quantization of x. Obviously such an assumption is valid only if the quantization used is fine enough. An investigation of the necessary quantization was given by Reiss (1974).

It should be emphasized, however, that the above described discretization of the model parameters is just a computation tool and has nothing to do with the continuous nature of the probability calculations method for the Monte Carlo simulation technique presented here.

In the course of calculations two assumptions were made:

(1) $f_1(x) > f_2(x)$ (for method of characteristics only).
(2) A phase flows in one direction only. Flow cannot reverse in the middle of the system. (A reversing flow can, however, be modeled by a positive phase and a negative phase, with an infinite exchange coefficient between them at the point of reversal.)

Several runs by both methods were made, for the fluidized bed example, in order to study the effect of the following factors:

(a) constant vs. varying coefficients;
(b) rate of change of the varying coefficients;
(c) effect of running more particles in the Monte Carlo simulation technique.

The ability of the Monte Carlo simulation method to describe spatial material distribution in the system was studied as well.

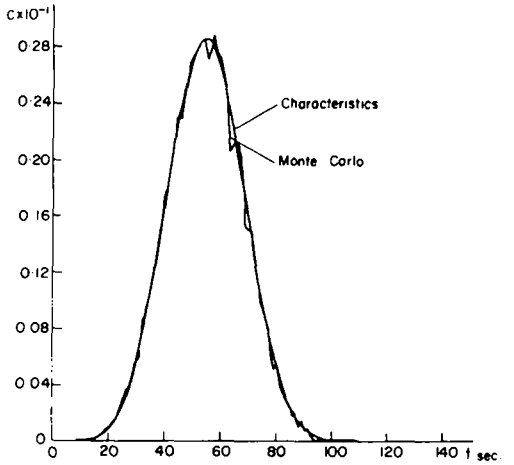

Figure 4. Fluidized bed, constant coefficients case.

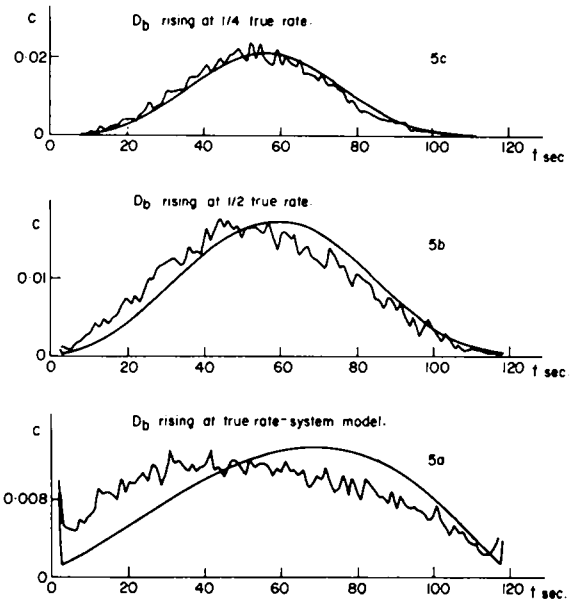

Figure 5. Comparison of Monte Carlo and characteristics for different rates of change of f and λ.

The first curve (figure 4) was obtained by both methods for the constant coefficient case. The system of table 1 with constant bubbles diameter $d_{br} = 2$ cm (size of bubbles remained constant implies constant velocities and constant exchange coefficients along the bed) and $u_o/u_{mf} = 2$ yielded practically identical RTD curves with $\bar{t} = 55.1$ sec and $\sigma = 13.7$ sec. Both methods can handle this case adequately. Being smoother the characteristic results may be preferable for such a case (see also Dayan & Levenspiel 1970). When solved for the varying parameters case, i.e. fluidized bed uf table 1, where bubble diameter changes (following [33]) and $u_o/u_{mf} = 2$, discrepancies appeared between the results of the two methods (see figure 5a). The moments of the distribution were:

Monte Carlo : $\bar{t} = 55.1$; $\sigma = 29.0$ (sec)
Characteristics: $\bar{t} = 63.44$; $\sigma = 26.4$.

To investigate this further, the top two plots in figure 5 (5b and 5c) show the results for the fluidized bed model with the linear regression for d_b taken at 1/4 (5c) and 1/2 (5b) of its slope in the model of [33].

We see that the divergence in results is much smaller for systems whose parameters vary less strongly than our fluidized bed.

Notice that the shape of the RTD changes for the model where the initial and final peaks are well defined. This is explained by the inability of the characteristics integration program (see Reiss (1974)) to handle what amounts to a delta function.

In addition, the integration method for the characteristics program gives a cumulative error which apparently gives a value which is too low.

The effect of running more particles in the Monte Carlo method was investigated by generating RTD curves; first based on 5000 particles and then on 24,000. The curves are given in figure 6 and the moments are:

$R = 5000$ particles : $\bar{t} = 55.3$; $\sigma = 28.8$ (sec)
$R = 24{,}000$ particles: $\bar{t} = 55.1$: $\sigma = 29.1$.

The Monte Carlo method obviously gives more reliable results when more particle trajectories are computed. We see in figure 6 that increasing the number of particles from 5000 to 24,000, considerably smoothens the resulting RTD.

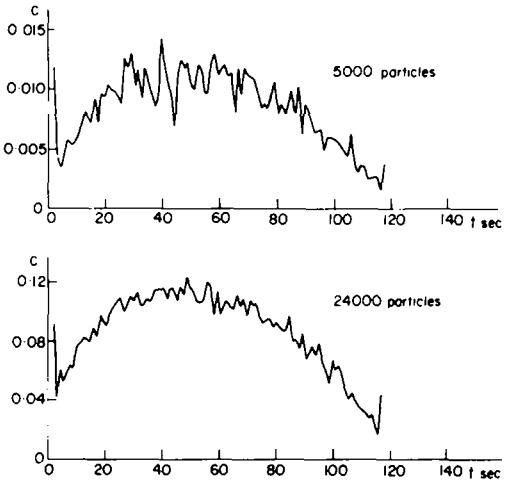

Figure 6. Effect of number of particles—Monte Carlo.

Thus, the number of particles necessary for the Monte Carlo solution depends on the desired smoothness and accuracy of the results. Figure 6 may be used as a guide for the effect of the number of particles. If only an indication of the expected residence time and its standard deviation is desired, a relatively small (1000) number of particles should be sufficient. A limit here is the randomness of the random number generator in the computer, which should, however, be sufficient for most applications.

To demonstrate the ability of the Monte Carlo simulation technique, to describe the spatial distribution of material within the system, particles concentrations were calculated for different values of t. Figure 7 shows the distribution along the system at 10, 20, 30, and 40 sec from time of injection. The tracer, or for that matter the particles, initially concentrated near $x = 0$, move up through the system towards $x = 100$.

However, for the determination of the particle distribution within the system, the characteristics program may be preferable if the distributions are desired for a large number of time values, as this is a natural product of the integration of the concentrations. The results of the Monte Carlo program in this case are less dependable, since the particle distribution at a given time must be derived by retracing the particle trajectories, which are always generated until the next projected jump point. The trajectories must, therefore, be retraced from the jump time to the time which we wish to sample. This adds an extra interpolation which reduces the accuracy of the results. (For example, four samplings of the particle distributions in the system (figure 7) changed the computed maximum residence time from 118 to 124 sec.) Unfortunately, the accuracy of the characteristics program is limited by the rate of change of the system parameters as was shown above.

It has been mentioned above that the program for the method of characteristics, in its present form, is unable to handle the case of countercurrent flow of phases with changing coefficients. The Monte Carlo method, however, can easily solve for both countercurrent and recycling flow (which is the case in our fluidized bed example) as well as for the fluidized bed of table 1 with $u_o/u_{mf} = 14$, which resulted in countercurrent (recycling) flow system.

A few words should be said about the two programs themselves. In the present form the Monte Carlo program requires more computer memory than the method of characteristics program. However, with a small modification in the Monte Carlo program, computer storage requirements of the two programs would be equivalent (Reiss 1974).

The storage requirements for the program as written are approximately $13N + 1.1R$, where N is the number of quantization levels and R is the number of particles run. With some minor modifications the storage requirements can be reduced to only $13N$. The characteristics program, in comparison, requires approximately $15N$ storage locations within the computer.

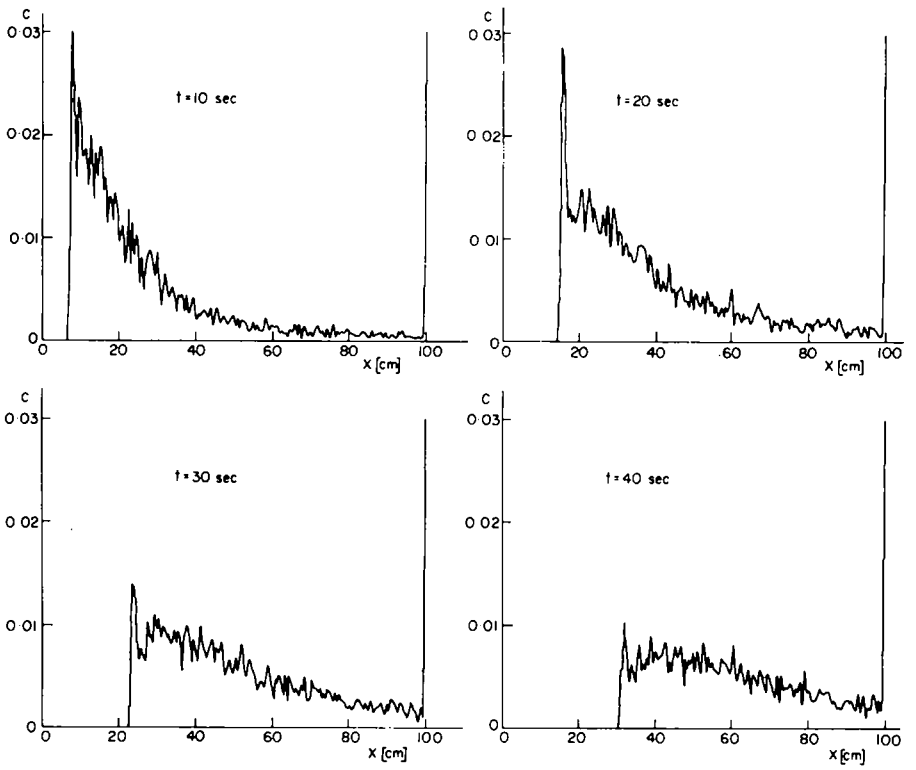

Figure 7. Particle distribution in the system.

On the other hand, the Monte Carlo Program takes less computer time to run than the method of characteristics.

In a typical computer run for the fluidized bed (10,000 particles, IBM370/165 Computer), the characteristics program ran for 70 sec, while the Monte Carlo program ran for only 30 sec. The time required for the characteristics program varies with N^2 (N quantizations for x and N quantizations for t), while the time for the Monte Carlo program varies linearly with the number of particles and the dependence on N is only secondary (the computation of the N sized tables is made only once, and the repeated search of these tables is by successive binary partition and so varies with $\log_2 N$). For fine quantization solutions of the RTD it is thus preferable to use the Monte Carlo program.

We note that there is widespread use of the popular dispersed plug flow model for describing flow systems that can be very adequately described by multiphase plug flow with varying coefficients (see, for example, the possible model for spouted bed suggested by Dayan *et al.* (1973)). Use of the dispersed plug flow model for such systems is made because of the computational difficulties arising in the solution of the hyperbolic partial differential equations obtained for the pure plug flow model. (The dispersed plug flow model usually results in a set of parabolic equations, easily solved by familiar numerical methods.) In

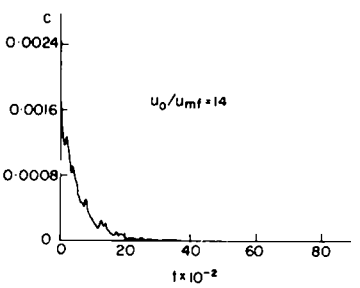

Figure 8. RTD in fluidized bed countercurrent case.

other words, inserting a diffusion term was not always made on the basis of physical reasons but as an escape from mathematical difficulties. It seems that with the aid of the present proposed stochastic technique it would be possible to solve the original simpler and more logical model describing such systems.

REFERENCES

DAVIDSON, J. & HARRISON, D. 1963 *Fluidized Particles*. Cambridge University Press, New York.

DAYAN, J. 1968 Dispersion with Adsorption in Packed Beds and Residence Time Distribution in Fluidized Beds, pp. 68–161. Doctoral Thesis, Illinois Institute of Technology.

DAYAN, J. & LEVENSPIEL, O. 1970 RTD for flow models with cross flow between plug-flow regions, *Chem. Engng Prog. Symp. Series* **66**, 28–36.

DAYAN, J., RAPPAPORT, D. & REISS, J. 1973 Residence time distribution of gas in spouted beds and in fluidized beds (Technion Publication TME-180), *4th Joint Chemical Engineering Conference, International Symposium on Spouted Beds*. Paper No. 37a, Vancouver, Canada.

FRYER, C. & POTTER, O. E. 1972 Bubble size variation in two-phase models of fluidized bed reactors. *Powder Technology* **6**, 317–322.

HIMMELBLAU, D. M. 1970 *Process Analysis by Statistical Methods*. Wiley, New York.

KATO, K. & WEN, C. Y. 1969 Bubble assemblage model for fluidized bed catalytic reactors. *Chem. Engng Sci.* **24**, 1351–1369.

KOBAYASHI, H. & ARAI, F. 1964 Paper presented at the 4th Symposium on Chemical Reaction Engineering, Soc. Chem. Engrs. (Japan), Osaka.

KOBAYASHI, H., ARAI, F. & CHIBA, T. 1966 Behavior of bubbles in a gas-solid fluidized bed. *Kag. Kog.* (English edition) **4**, 147–153.

KUNII, D. & LEVENSPIEL, O. 1969 *Fluidization Engineering*. Wiley, New York.

ORCUTT, J. C. 1960 Ph.D. Thesis, University of Delaware.

RAPPAPORT, D. & DAYAN, J. 1974 Probabilistic models for tracer distribution in multiphase flow systems. *J. Statistical Phys.* **11** (to appear).

REISS, J. 1974 Residence Time Computations for Transport Processes in Non-homogeneous Media. Master Thesis, Technion, Electrical Engineering Department.

YOSHIDA, K. & KUNII, D. 1968 Stimulus and response of gas concentration in bubbling fluidized beds. *J. Chem. Engng Japan* **1**, 11–16.

Résumé—On présente une nouvelle technique de simulation de Monte Carlo, continue sur le temps et l'espace, pour résoudre les équations décrivant la distribution d'un traceur dans des écoulements multiphasiques non homogènes à bouchons. On donne une comparaison avec la méthode des caractéristiques, couramment utilisée. Cette comparaison indique que la méthode des caractéristiques n'est pas fiable pour des systèmes dans lesquels les paramètres varient de façon particulière. De plus les résultats indiquent que la méthode de Monte Carlo suggérée est plus efficace en temps de calcul que la méthode des caractéristiques. On donne des exemples.

Auszug—Fuer die Loesung von Gleichungen, die die Indikatorenverteilung in nichthomogenen Vielphasensystemen mit Pfropfenstroemung beschreiben, wird eine neue, zeitlich und raeumlich kontinuierliche Monte Carlo-Simulationstechnik angegeben. Beim Vergleich mit der ueblicherweise angewandten Charakteristikenmethode erweist es sich, dass letztere bei Systemen mit speziell veraenderlichen Parametern unzuverlaessig ist. Ferner zeigen die Ergebnisse, dass die vorgeschlagene Monte Carlo- Technik Rechnerzeit wirkungsvoller ausnuetzt, als die Charakteristikenmethode. Beispiele werden angefuehrt.

Резюме—Предложена модель типа метода Монте-Карло с непрерывным временем и пространством для решения уравнений, описывающих распределение меченых атомов в многофазных неоднородных системах. Проведено сравнение с известным методом характеристик. Сравнение показало, что для систем со специально меняющимися параметрмн, метод характеристик является ненадежным. Было показано, что предлагаемая техника Монте-Карло является ъолее аффективной. Приведены примеры.